AIP | Review of Scientific Instruments

Electrostatic energy harvesting device with dual resonant structure for wideband random vibration sources at low frequency

Yulong Zhang, Tianyang Wang, Ai Zhang, Zhuoteng Peng, Dan Luo, Rui Chen, and Fei Wang

Citation: Review of Scientific Instruments **87**, 125001 (2016); doi: 10.1063/1.4968811
View online: http://dx.doi.org/10.1063/1.4968811
View Table of Contents: http://scitation.aip.org/content/aip/journal/rsi/87/12?ver=pdfcov
Published by the AIP Publishing

Electrostatic energy harvesting device with dual resonant structure for wideband random vibration sources at low frequency

Yulong Zhang,[1] Tianyang Wang,[1] Ai Zhang,[1] Zhuoteng Peng,[1] Dan Luo,[1] Rui Chen,[1] and Fei Wang[1,2,a)]

[1]*Department of Electrical and Electronic Engineering, Southern University of Science and Technology, Shenzhen 518055, China*

[2]*Shenzhen Key Laboratory of 3rd Generation Semiconductor Devices, Shenzhen 518055, China*

(Received 20 May 2016; accepted 13 November 2016; published online 5 December 2016)

In this paper, we present design and test of a broadband electrostatic energy harvester with a dual resonant structure, which consists of two cantilever-mass subsystems each with a mass attached at the free edge of a cantilever. Comparing to traditional devices with single resonant frequency, the proposed device with dual resonant structure can resonate at two frequencies. Furthermore, when one of the cantilever-masses is oscillating at resonance, the vibration amplitude is large enough to make it collide with the other mass, which provides strong mechanical coupling between the two subsystems. Therefore, this device can harvest a decent power output from vibration sources at a broad frequency range. During the measurement, continuous power output up to 6.2-9.8 μW can be achieved under external vibration amplitude of 9.3 m/s^2 at a frequency range from 36.3 Hz to 48.3 Hz, which means the bandwidth of the device is about 30% of the central frequency. The broad bandwidth of the device provides a promising application for energy harvesting from the scenarios with random vibration sources. The experimental results indicate that with the dual resonant structure, the vibration-to-electricity energy conversion efficiency can be improved by 97% when an external random vibration with a low frequency filter is applied. *Published by AIP Publishing.* [http://dx.doi.org/10.1063/1.4968811]

I. INTRODUCTION

In the past decade, energy harvesting from kinetic energy sources in the ambient environment has attracted much interest from both academia and industry, as a promising way to replace the traditional batteries providing sustainable energy for self-powered wireless electronics.[1–3] There are many types of kinetic energies available in the environment, such as machinery vibrations from automobiles and airplanes, structural vibrations from bridges and buildings, or human motions. In some applications, the vibration source may behave at a specific oscillating frequency, while more commonly the frequency spectrum of the vibration source can be quite random,[4] which is a big challenge for the energy harvesting efficiency.

There are a few solutions for vibration-to-electricity conversion naming as electromagnetic,[5,6] piezoelectric,[7–10] triboelectricity,[11,12] and electrostatic principles.[13–16] Based on these principles, induced current or induced charges can be generated when a proof mass vibrates according to the external excitation. Generally, electromagnetic induction requires bulky device size since the power output decreases dramatically when the coil area and turning number are limited. For piezoelectric energy harvesters, lead zirconate titanate (PZT) material is widely used to achieve a decent piezoelectric constant, while process compatibility of PZT should be concerned for mass production and system integration with MEMS. Triboelectricity has attracted much attention recently as electricity can be generated simply by the contact and separation between two materials. However, the wear of the contact surfaces has not been well studied and therefore the lifetime of the devices might be an issue. Unlike the previous methods, electrostatic energy harvester utilizes a compact design typically working under the non-contact mode without friction or wear, where electret materials and MEMS compatible process are often applied.[17–21] A comprehensive review on the electret based energy harvester has been provided by Suzuki in 2011.[22]

In order to maximize the output power of the energy harvester, most of the previous researchers utilized linear harmonic structure possessing a resonant frequency to match the external excitation frequency. Unfortunately, the performance of the energy harvester will decrease to a large extent when the external excitation frequency shifts off the resonant frequency of the device. In practice, it is difficult to exactly match the resonant frequency of the final device with the design according to the fabrication errors. On the other hand, the vibration frequency in the environment is varying or distributing in a wide spectrum range, as mentioned above. To overcome this limitation, a great effort has recently been made to broaden the bandwidth of the device.[23–32] The state-of-the-art techniques for energy harvesters based on electromagnetic, piezoelectric, and triboelectric principles cover tuning resonance frequency,[23,24] multimodal energy harvesting,[25,26] frequency up-conversion,[27,28] and exploiting nonlinear oscillations.[29] For instance, Lin *et al.*[30] implement a multi-cantilever piezoelectric generator with current standard MEMS fabrication techniques, which the resonance frequencies of the device possess between 237 Hz and 244.5 Hz. The bandwidth of electrostatic

a)Author to whom correspondence should be addressed. Electronic mail: wangf@sustc.edu.cn

energy harvesters has been studied by introducing a repulsive electrostatic force[14] and by gap-spacing control with a mechanical stopper.[16]

In our previous work,[33] we have developed a micro-electrostatic energy harvester with out-of-the-plane gap closing scheme based on the advanced MEMS technology. We have discovered that the bandwidth of the energy harvester can be tuned from 4.6 Hz to 20.0 Hz when the vibration amplitude increases from 0.05 g to 1 g. In this paper, we propose a dual resonant structure for a broadband electrostatic energy harvester, which consists of two cantilever-mass subsystems. The harvester is based on a variable capacitor structure, whose capacitance changes when the gap distance between the two electrodes of the capacitor varies in response to an external vibration source. With this structure, we have experimentally verified the broadening of the bandwidth of the energy harvester. Furthermore, we have applied this prototype device for energy harvesting from random vibration sources at a low frequency spectrum. The measurements have shown a larger power output comparing to the conventional single resonant structures, which provides more promising applications.

II. PRINCIPLE AND SIMULATION

For a linear spring-mass system driven by an external vibration source shown in Fig. 1(a), the vibration amplitude of the proof mass X_m can be many times larger than the amplitude of the vibration source Y_m. At resonance, we can have $X_m = QY_m$, where Q is the quality factor of the system. For instance, when a vibration source is applied with acceleration amplitude of 1 g (9.8 m/s^2) at a low frequency of 50 Hz, Y_m is approximately 0.1 mm; therefore, the maximum vibration amplitude of the proof mass X_m can be estimated as 10 mm if the quality factor Q of the system is 100. This large vibration amplitude cannot be fully utilized concerning the small size of the energy harvesting device.

In this paper, we propose a dual resonant structure using two stainless steel cantilevers and two masses for the prototype electrostatic energy harvester, as shown in Fig. 1(b). When one of the cantilever-masses is oscillating at resonance, the vibration amplitude is large enough to make it collide with the other mass, which provides strong mechanical coupling between the two subsystems. Thanks to the mechanical coupling, the latter cantilever-mass is driven to the forced vibration mode. Therefore, it can also oscillate to a decent level even though the frequency of the external excitation is off its resonant frequency. When the difference of resonance frequencies of two cantilever-mass subsystems is optimized, the power output between the two resonance frequencies will be increased. As shown in Fig. 1(c), this collision coupling effect of the dual resonant system will take advantage of both the subsystems to broaden the bandwidth of the device.

The mechanical part of the electrostatic energy harvesting device is analyzed as a mass-spring system as shown in

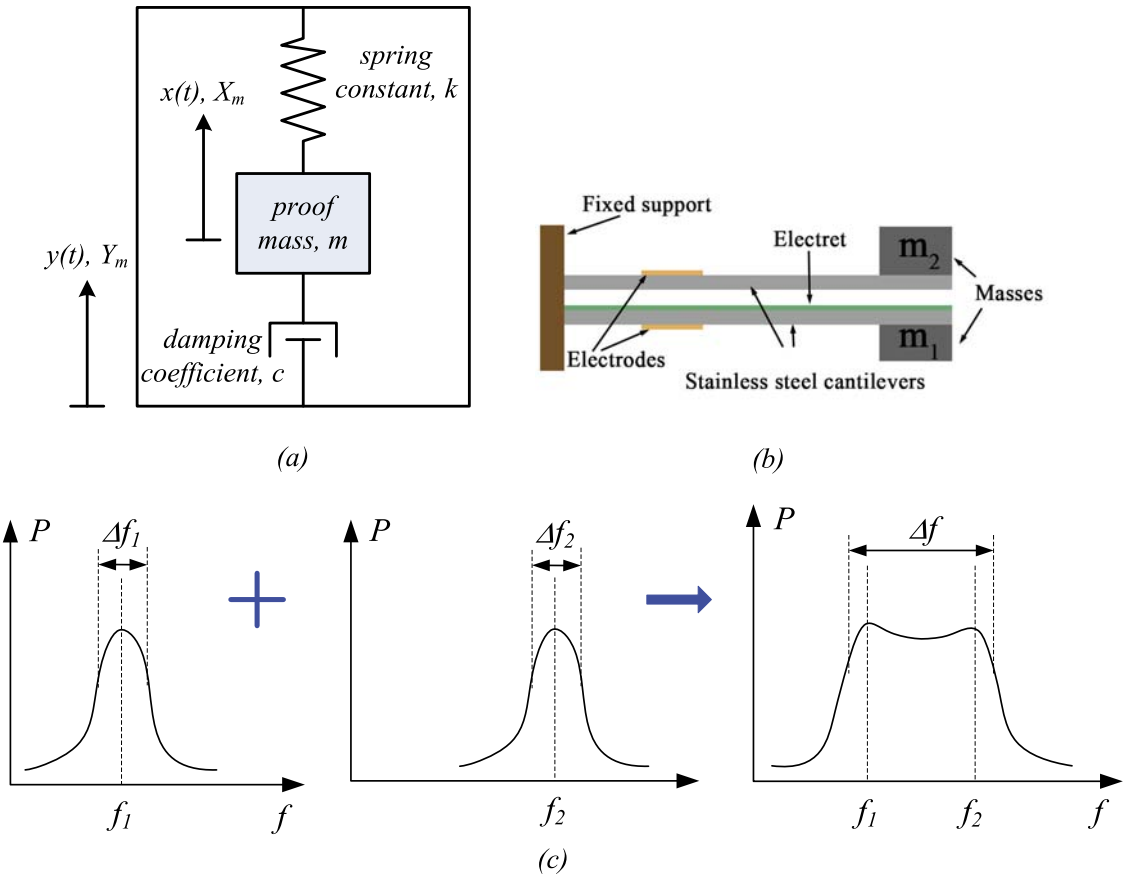

FIG. 1. (a) Mechanical model of a vibration energy harvester with proof mass m, spring constant k, and damping coefficient c; (b) schematic of the electrostatic energy harvesting device with a dual resonant structure; (c) frequency response of the energy harvesting devices with single cantilever (left, middle) and the energy harvesting device with dual resonant cantilevers (right).

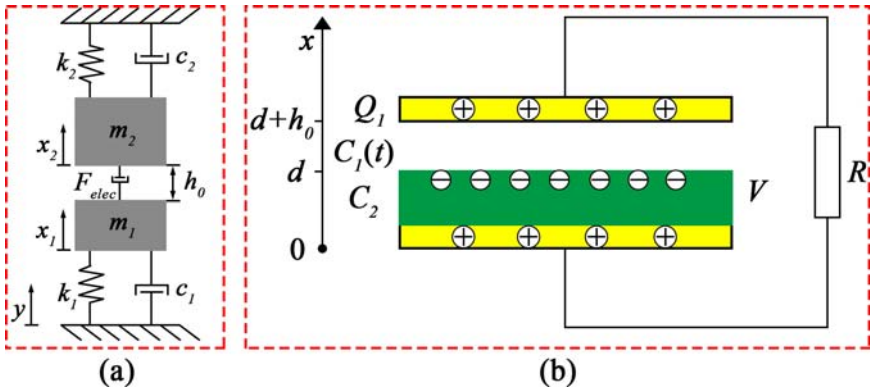

FIG. 2. (a) The mechanical model and (b) the electrical model of the electrostatic energy harvesting device.

Fig. 2(a). Generally, the mechanical performance of the mass-spring-damper system without collision can be written as

$$\begin{cases} m_1(\ddot{y} + \ddot{x}_1) + c_1\dot{x}_1 + k_1x_1 + m_1g - F_{elec} = 0, \\ m_2(\ddot{y} + \ddot{x}_2) + c_2\dot{x}_2 + k_2x_2 + m_2g + F_{elec} = 0, \end{cases} \quad (1)$$

where y and $x_{i(i=1,2)}$ are the displacement of the external vibration source and the relative displacement of the mass, $m_i(i = 1,2)$ is the mass, $k_i(i = 1,2)$ and g are the stiffness of the spring structure and the gravitational acceleration, $c_i(i = 1,2)$ is the coefficient of viscous damping force,[34] and F_{elec} is the electrostatic transduction force, respectively. The colliding force could be further included in Eq. (1) when the external acceleration amplitude is large enough to trigger the collision between the two masses.[35] Then, the differential equation for the motion of masses in the dual resonant cantilever system can be described by

$$\begin{cases} m_1(\ddot{y} + \ddot{x}_1) + c_1\dot{x}_1 + k_1x_1 + m_1g - F_{elec} + F_c = 0, \\ m_2(\ddot{y} + \ddot{x}_2) + c_2\dot{x}_2 + k_2x_2 + m_2g + F_{elec} - F_c = 0, \end{cases} \quad (2)$$

where F_c is the colliding force between the two proof masses. The colliding force should be proportional to the elastic deformation of the beams, which can be defined by an effective spring constant of the collision, k_c,

$$F_c = \begin{cases} -k_c\,(h_0 - x_1 + x_2), & \text{for } h_0 - x_1 + x_2 < 0 \\ 0, & \text{for } h_0 - x_1 + x_2 \geq 0 \end{cases}. \quad (3)$$

Figure 2(b) shows the electrical scheme of the electrostatic energy transduction principle using an electret. According to the Kirchhoff's laws, the differential equation governing the electrostatic system is expressed by,[36]

$$R\frac{dQ_1}{dt} = V - Q_1\left[\frac{1}{C_1(t)} + \frac{1}{C_2}\right], \quad (4)$$

where Q_1, R, and V stand for the induced charge on the upper electrode, the external load resistance, and the surface potential of the pre-charged electret, respectively, $C_1(t)$ and C_2 correspond to the capacitance of the air gap and that of the electret dielectric material, respectively.

Based on the analysis above, we have solved the system numerically in Matlab/Simulink software. Figure 3 shows the simulated power output which can be harvested from vibration sources at frequency ranging from 32 Hz to 55 Hz with different vibration amplitudes. When the vibration amplitude is lower than 2.6 m/s^2, there is no collision between the two masses. Therefore, there are two separated power output peaks at $f = 37$ Hz and $f = 45$ Hz in the spectrum plot which correspond to the resonant frequencies of the two subsystems, respectively. The power output is significantly low when we apply a vibration source with frequency between the two resonant frequencies. When the vibration amplitude is increased to 5.3 m/s^2, the two masses will collide with each other and therefore the mechanical coupling effect between the two subsystems is enhanced. As shown in Fig. 3, the frequency response of the device shows a flat plateau spectrum for the power output. The device can also harvest a decent energy at the vibration frequency between the two resonant frequencies. The improved frequency response of the device will increase the energy harvesting efficiency from vibration sources with a random frequency. A similar model for the mechanical coupling effect of piezoelectric energy harvesting device has been described in more detail in Ref. 8.

III. EXPERIMENTS

Generally, an electrostatic energy harvester consists of two electrodes. One electrode can be arranged on the cantilever and the other one on a fixed plate. As shown in Fig. 4, the counter electrode of the device with a single cantilever is fixed

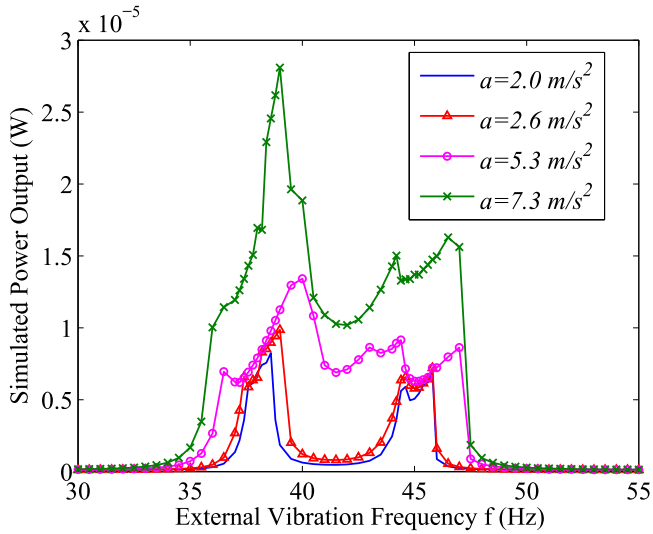

FIG. 3. Simulated power output as a function of the external vibration frequency.

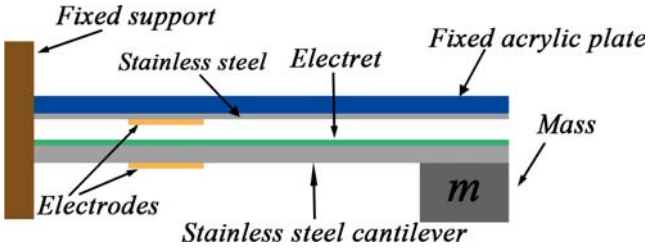

FIG. 4. Schematic of the electrostatic energy harvesting device with single cantilever.

on an acrylic plate. With this scheme, the bandwidth of the energy harvesting device can be broadened at a cost of the maximum power output. Here in this paper, we propose an electrostatic energy harvester which consists of a dual resonant structure with two cantilevers. Figure 1(b) shows the device with the dual resonant structure, consisting of two cantilevers made of stainless steels, where at the tip of each stainless steel a proof mass is mounted. CYTOP polymer (CTL-809M from Asahi Glass) is used as an electret material covered in the surface of bottom stainless steels.[11] The two stainless steels are separated by a spacer slice. As shown in Fig. 5, the device is mounted on a mechanical shaker (Brüel & Kjær, 4810) with a reference accelerometer to monitor the acceleration, and driven by the excitation signal generated from a signal generator (Brüel & Kjær, LAN-XI 3160) and a power amplifier (Brüel & Kjær, 2719). Some key parameters for the device are listed in Table I.

The power output of the energy harvesting device is dependent on the external load resistance. First, the optimal load for the energy harvesting device is tested when an external sinusoidal vibration is applied at a frequency of 37 Hz, with a root mean square (RMS) acceleration of 2.5 m/s^2. The RMS power output is measured when the external load resistance is tuned during the measurement. Figure 6 shows the relationship between the RMS power output and the external load resistance. With an optimal load of about 16 MΩ, maximum RMS power of 1.65 μW is harvested from the low amplitude vibration. All the measurements in Sec. IV are performed with the same external load of 16 MΩ unless otherwise noted.

The two devices with single cantilevers as shown in Fig. 4 (with L_1, w_1, d_1, m_1 for device 1 and L_2, w_2, d_2, m_2 for device two) are also tested under sinusoidal excitation signals

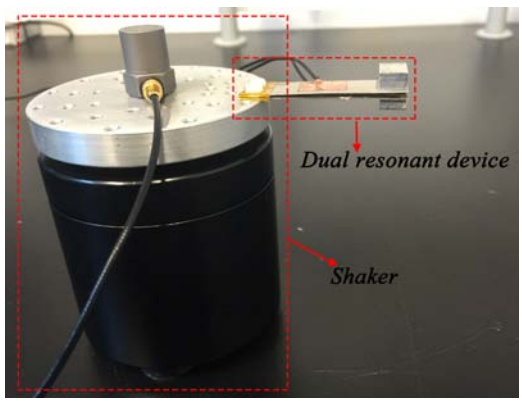

FIG. 5. The electrostatic energy harvesting device with a dual resonant structure is mounted on a shaker.

TABLE I. Parameters of the electret-based energy harvesting device with a dual resonant structure.

Parameters	Value	Description
L_1, L_2	5.0 cm	Stainless steel length
w_1, w_2	1.5 cm	Stainless steel width
d_1, d_2	0.2 cm	Stainless steel thickness
m_1	1.14 g	Bottom mass
m_2	0.83 g	Top mass
h_0	0.2 cm	Initial gap between two stainless steels
V	−950 V	Surface potential of electret after corona charging

for comparison. Figure 7 plots the RMS power outputs as a function of the frequencies of the external vibration source. For both devices, maximum power output can be achieved when the vibration is applied at the resonant frequency of the devices (f_0 = 39.3 Hz for device 1 and f_0 = 47.5 Hz for device 2, respectively), with an amplitude of lower than 2.8 m/s^2. As the acceleration amplitude of the external vibration increases from 1.4 m/s^2 to 2.8 m/s^2, the vibration amplitudes of the proof masses increase accordingly and therefore, collision occurs between the cantilever and fixed plate electrode with excitation larger than 2.8 m/s^2. The frequency response exhibits a broad operating bandwidth near its resonant frequency. The operating bandwidths widen to frequency ranges of 6.9 Hz (36.9–43.8 Hz in Figure 6(a) for device 1) and 6.0 Hz (45.7–51.7 Hz in Fig. 7(b) for device 2) at an acceleration of 9.8 m/s^2 (1 g) for the two devices with single cantilever, respectively.

The frequency response of the dual resonant cantilever device (shown in Fig. 4) is characterized with the sinusoidal excitation signals ranging from 30 Hz to 55 Hz at constant RMS accelerations from 1.3 m/s^2 to 9.3 m/s^2. As shown in Fig. 8, with a vibration source at acceleration amplitude lower than 1.3 m/s^2, two separated power peaks are achieved at the resonant frequencies of the subsystems. The power output of

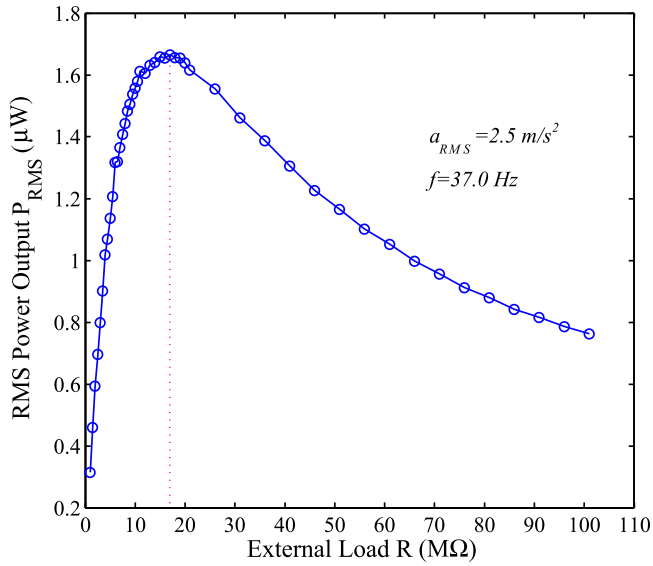

FIG. 6. The RMS power output when the external load increases from 1 MΩ to 101 MΩ at the RMS acceleration of 2.5 m/s^2 where the external sinusoidal vibration frequency is 37.0 Hz.

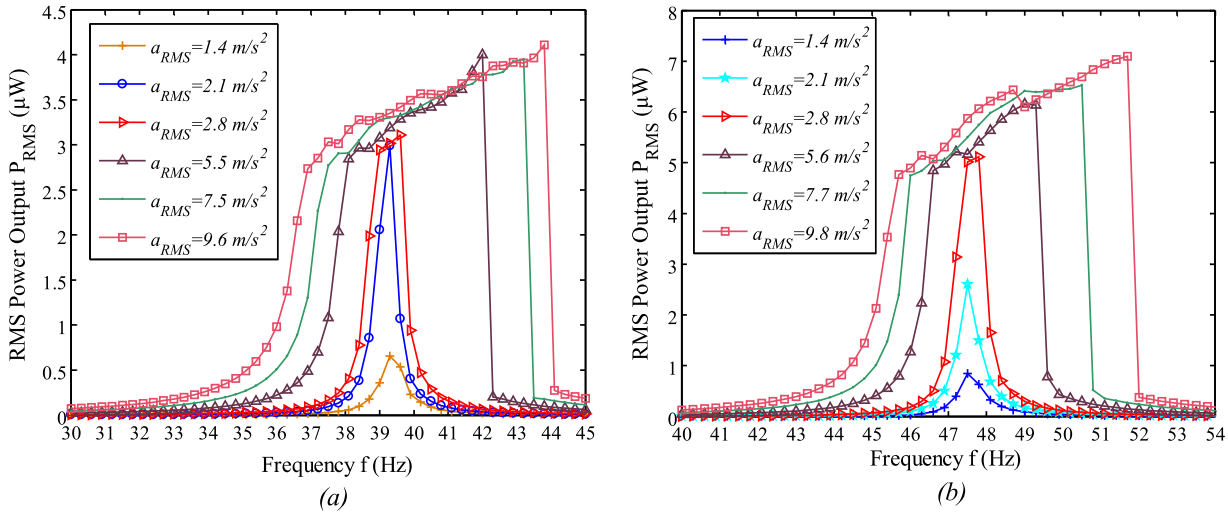

FIG. 7. Experimental results of RMS powers vs frequencies of single cantilever at different accelerations: (a) Resonance frequency of 39.3 Hz; (b) resonance frequency of 47.5 Hz.

the device is low at the frequency range between the two resonant frequencies because no collision occurs at low acceleration amplitude. When the acceleration amplitude is increased, the resonant frequencies of the device are slightly increased, which is mainly due to the "hardening effect" of the cantilevers. Moreover, the bandwidth of each subsystem is broadened with larger acceleration amplitude, which is similar to the device with single cantilever. When a vibration source is applied with amplitude of acceleration larger than 9.3 m/s^2, the coupling effect between the two subsystems is strong enough that the energy harvesting device can always provide a decent power output (6.2-9.8 μW) at a broad frequency range of 12.0 Hz (36.3-48.3 Hz). Therefore, the bandwidth of the device is successfully broadened to about 30% of the central frequency of the device.

According to Mitcheson *et al.*,[1] the theoretical maximum power output P_{max} is $\sim Y_0 Z_l \omega^3$ m/2. Since there are two masses in the dual structure, we can take the overall mass ($m_1 + m_2$), and Z_l can be estimated as the initial gap of ~2 mm for the vibration frequency ranging from 35 Hz to 46 Hz with vibration amplitude of 7.3 m/s^2. Based on the above values, we have estimated the effectiveness of the device ranging from 0.12% to 0.19%, as shown in Fig. 9.

The up-sweep and down-sweep frequency responses of the device are further studied, respectively. As shown in Fig. 10(a), there is no collision between the two masses at a low acceleration of 1.3 m/s^2; therefore, two power output peaks both of about 4 μW are achieved at the resonance frequencies of 35.7 Hz and 44.5 Hz for the two cantilever-mass subsystems, respectively. Only a little discrepancy between the frequency up-sweep and down-sweep can be observed during this measurement. From the inset plot in Fig. 10(a), we can see that the voltage output has a waveform close to a sinusoidal function at a frequency of 40.5 Hz, which also indicates good linearity and weak coupling between the two subsystems at the frequency range between the two resonant frequencies.

When a high acceleration of 9.3 m/s^2 is applied as shown in Fig. 10(b), maximum power output of 9.8 μW can be harvested at the frequencies close to resonance. Besides, the power output at the frequency range between the two resonant

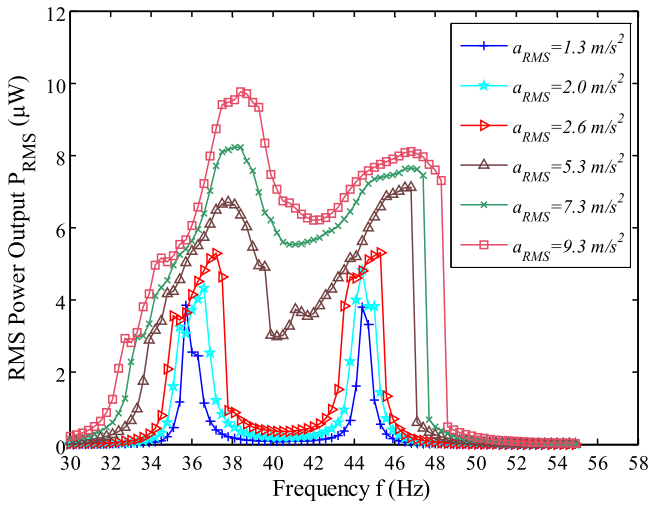

FIG. 8. Experimental results of RMS power output from the device with a dual resonant structure as a function of the external vibration frequency with vibration amplitude from 1.3 m/s^2 to 9.3 m/s^2.

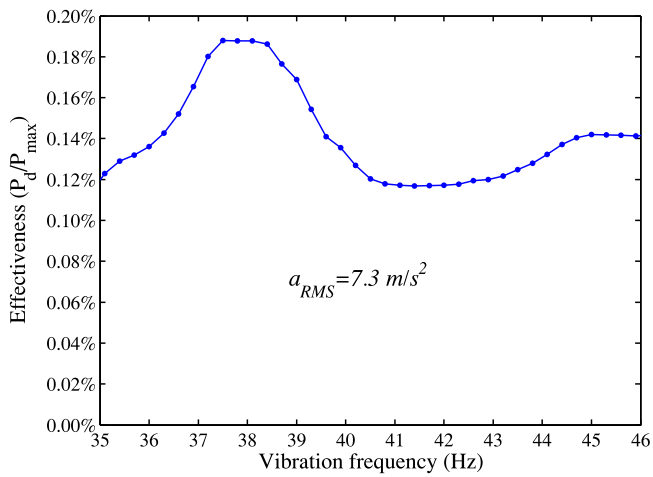

FIG. 9. Effectiveness of the dual resonant device for the vibration frequency ranging from 35 Hz to 46 Hz with amplitude of 7.3 m/s^2.

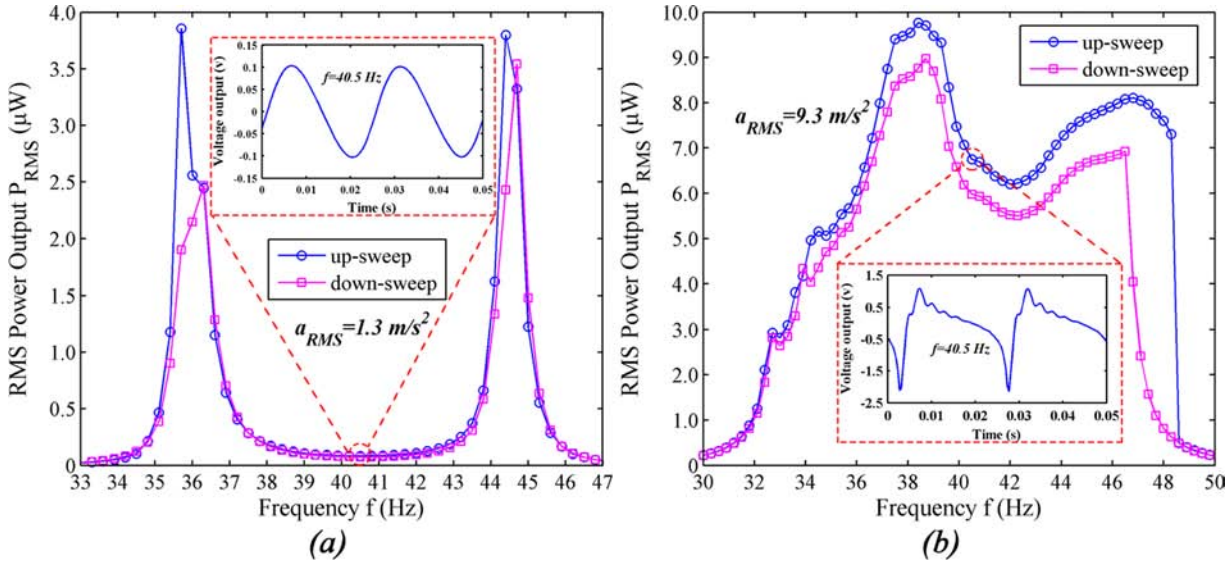

FIG. 10. Experimental results of RMS powers vs frequencies of the dual resonant structure with vibration amplitude of (a) 1.3 m/s^2, and (b) 9.3 m/s^2, respectively. The inset plots show the waveform of the voltage output under an external vibration frequency of 40.5 Hz for both cases.

frequencies can be significantly improved, thanks to the collision between the two subsystems. The inset plot in Fig. 10(b) shows the asymmetric waveform of the voltage output at a frequency of 40.5 Hz, which indicates the nonlinearity and strong coupling effect from the collision. It should also be noted that an obvious discrepancy between the frequency up-sweep and down-sweep can be seen from the measurement according to the collision coupling effect.

The broad bandwidth of the device with dual resonant structure provides a promising application on the energy harvesting from random vibration sources at a low frequency. The response on random vibrations of the dual resonant device,

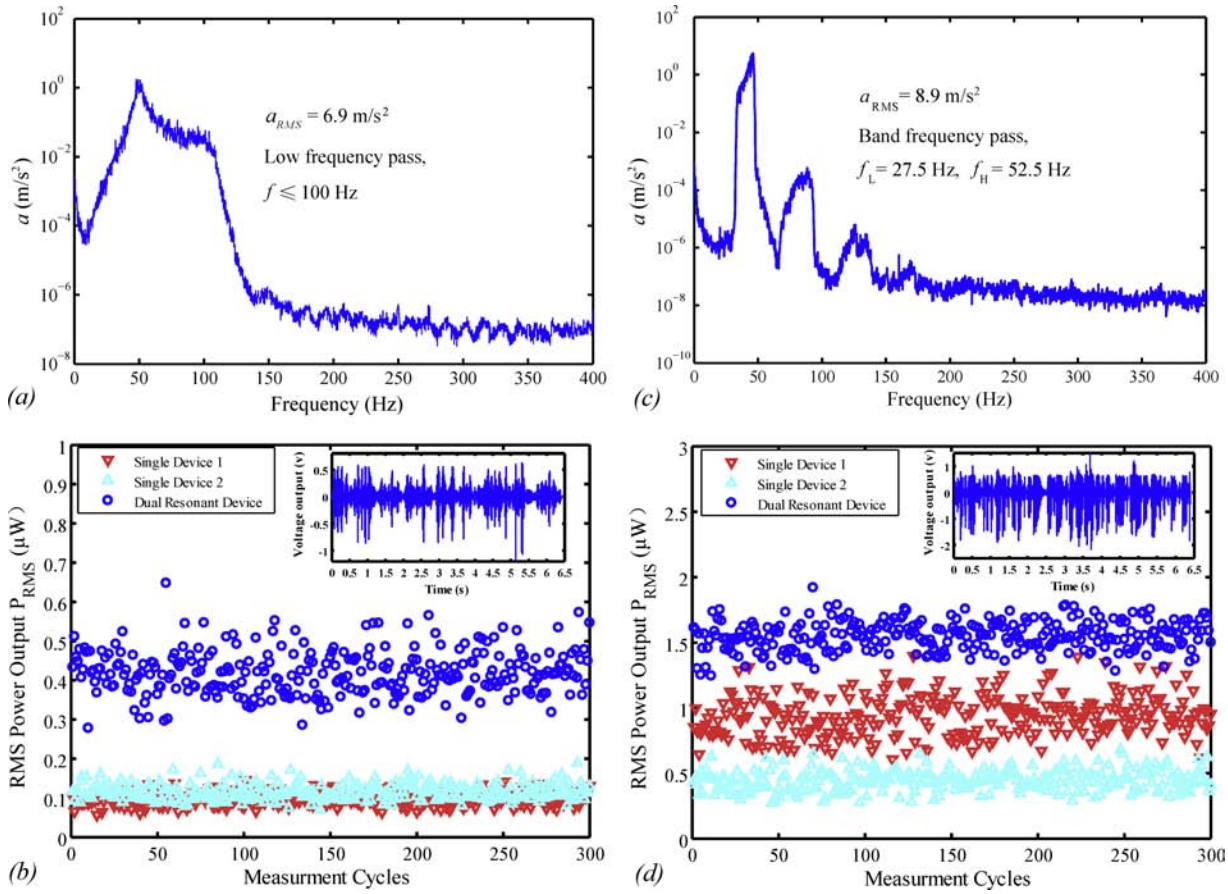

FIG. 11. RMS power output of the dual resonant device, single cantilever device 1, and single cantilever device 2 under random vibrations with ((a) and (b)) lowpass filter ($f \leq 100$ Hz) and ((c) and (d)) bandpass filter ($f = 40 \pm 12.5$ Hz). The inset plots show the real time voltage output under the two random vibration sources.

TABLE II. Vibration sources and measurement results.

Vibration sources	Lowpass filter	Bandpass filter
Acceleration amplitude (a_{rms})	6.9 m/s^2	8.9 m/s^2
Power output from device 1 (P_1)	0.097 μW	0.941 μW
Power output from device 2 (P_2)	0.116 μW	0.444 μW
Power output from dual device (P_d)	0.420 μW	1.549 μW
$P_d/(P_1 + P_2)$	1.97	1.12

single cantilever device 1, and single cantilever device 2 is characterized for 300 cycles with 6.4 s/cycle under the same external random excitation signals. Figure 11(a) shows the frequency spectrum of the vibration source from a lowpass filter (at frequency lower than 100 Hz), and the RMS power outputs of the three devices harvested from the random vibration are shown in Fig. 11(b). Another random vibration source from a bandpass filter (at a center frequency of 40 Hz with a bandwidth of 25 Hz) is shown in Fig. 11(c) with the RMS power outputs plotted in Fig. 11(d).

It should be noted that the overall power output of the device with a dual resonant structure is a few times larger than that of the single device when a sinusoidal vibration source at a specific frequency is applied, as shown in Fig. 8. However, the increase of the power output seems less significant from the vibration source with a random frequency. This is mainly due to the fact that, the oscillation amplitudes of the proof masses are much smaller when driven by random vibration than those by a sinusoidal vibration source, which provides less chance for the collision and mechanical coupling effect between the two masses. Furthermore, we have also noticed that the average power outputs of the bandpass measurements are higher than those of the lowpass measurements because the bandpass frequency spectrum fits better to the operating bandwidths of the three devices. The uniformity of the output voltage waveforms of the dual resonant device can also illustrate it, as shown in the inset graphs in Fig. 11. As shown in Figs. 7 and 8, the operating bandwidth of the dual resonant device is larger than the single cantilever devices 1 and 2, thus the power output of the dual resonant device (1.5 μW) is higher than those of the latter two devices (0.9 μW and 0.4 μW, respectively), as shown in Fig. 11(d). As summarized in Table II, the energy harvesting efficiency of the dual device is larger than the sum of the two single devices by 97% when random vibration sources with a low frequency filter are applied. For practical application where the vibration source has a certain frequency spectrum, the energy harvesting device can be optimized by tuning the resonant frequency of the two subsystems.

IV. CONCLUSIONS

We have proposed a broadband electrostatic energy harvesting device with a dual resonant structure. The dual resonant structure consists of two cantilever-mass subsystems, which are separated by a spacer slice. Electrical power is generated when the gap distance varies between the top and the bottom cantilevers driven by an external vibration source. Comparing to the single devices, the device with dual resonant structure exhibits broader bandwidth, thanks to the collision coupling effect between the two masses. The bandwidth of the device is successfully broadened to about 30% of the central frequency of the device, and RMS power output of 6.2-9.8 μW can be harvested in this broad frequency range when an external acceleration of 9.3 m/s^2 is applied. With the dual resonant device, the vibration-to-electricity energy conversion efficiency under random vibration sources can be significantly improved, which provides promising applications.

ACKNOWLEDGMENTS

This work is supported by National Natural Science Foundation of China (Project No. 51505209) and Science, Technology and Innovation Commission of Shenzhen Municipality (Projects Nos.: JCYJ20150930160634263, JCYJ20150827165024088, and KQTD2015071710313656). Fei Wang is also supported by Guangdong Natural Science Funds for Distinguished Young Scholar (Project No. 2016A030306042).

[1]P. D. Mitcheson, E. M. Yeatman, G. K. Rao, A. S. Holmes, and T. C. Green, "Energy harvesting from human and machine motion for wireless electronic devices," Proc. IEEE **96**(9), 1457–1486 (2008).
[2]S. P. Beeby, M. J. Tudor, and N. M. White, "Energy harvesting vibration sources for microsystems applications," Meas. Sci. Technol. **17**, R175 (2006).
[3]See http://www.microgensystems.com/ for information about the energy harvester products.
[4]S. Roundy, "Energy scavenging for wireless sensor nodes with a focus on vibration to electricity conversion," Ph.D. thesis, University of California, Berkeley, 2003. thesis.
[5]S. P. Beeby, R. N. Torah, M. J. Tudor, P. Glynne-Jones, T. O'Donnell, C. R. Saha, and S. Roy, "A micro electromagnetic generator for vibration energy harvesting," J. Micromech. Microeng. **17**(7), 1257–1265 (2007).
[6]N. N. H. Ching, H. Y. Wong, W. J. Li, P. H. W. Leong, and Z. Wen, "A laser-micromachined multi-modal resonating power transducer for wireless sensing systems," Sens. Actuators, A **97–98**, 685–690 (2002).
[7]S. Li, Z. Peng, A. Zhang, and F. Wang, "Dual resonant structure for energy harvesting from random vibration sources at low frequency," AIP Adv. **6**, 015019 (2016).
[8]S. Li, A. Crovetto, Z. Peng, A. Zhang, O. Hansen, M. Wang, X. Li, and F. Wang, "Bi-resonant structure with piezoelectric PVDF films for energy harvesting from random vibration sources at low frequency," Sens. Actuators, A **247**, 547–554 (2016).
[9]S. Roundy and P. K. Wright, "A piezoelectric vibration based generator for wireless electronics," Smart Mater. Struct. **13**(5), 1131 (2004).
[10]Q. Shi, T. Wang, T. Kobayashi, and C. Lee, "MEMS based piezoelectric ultrasonic energy harvester for self-powered under-water applications," in The 29th IEEE International Conference on Micro Electro Mechanical Systems (MEMS 2016), China, 24–28 January 2016.
[11]L. Dhakar, F. E. H. Tay, and C. Lee, "Development of a broadband triboelectric energy harvester with SU-8 micropillars," J. Microelectromech. Syst. **24**(1), 91 (2015).
[12]G. Zhu, Z. Lin, Q. Jing, P. Bai, C. Pan, Y. Yang, Y. Zhou, and Z. L. Wang, "Toward large-scale energy harvesting by a nanoparticle-enhanced triboelectric nanogenerator," Nano Lett. **13**(2), 847–853 (2013).
[13]H. Lo and Y. C. Tai, "Parylene-based electret power generators," J. Micromech. Microeng. **18**, 104006 (2008).
[14]Y. Suzuki, D. Miki, M. Edamoto, and M. Honzumi, "A MEMS electret generator with electrostatic levitation for vibration-driven energy-harvesting applications," J. Micromech. Microeng. **20**(10), 104002 (2010).
[15]A. Crovetto, F. Wang, and O. Hansen, "An electret-based energy harvesting device with a wafer-level fabrication process," J. Micromech. Microeng. **23**, 114010 (2013).
[16]T. Takahashi, M. Suzuki, T. Nishida, Y. Yoshikawa, and S. Aoyagi, "Vertical capacitive energy harvester positively using contact between proof mass and electret plate—Stiffness matching by spring support

of plate and stiction prevention by stopper mechanism," in *28th IEEE International Conference on Micro Electro Mechanical Systems (MEMS 2015)* (IEEE, 2015), pp. 1145–1148.
[17]T. Tsutsumino, Y. Suzuki, N. Kasagi, and Y. Sakane, "Seismic power generator using high-performance polymer electret," in *19th IEEE International Conference on Micro Electro Mechanical Systems (MEMS 2006)* (IEEE, Istanbul, 2006), pp. 98–101.
[18]Y. Sakane, Y. Suzuki, and N. Kasagi, "The development of a high-performance perfluorinated polymer electret and its application to micro-power generation," J. Micromech. Microeng. **18**(10), 104011 (2008).
[19]K. Kashiwagi, K. Okano, T. Miyajima, Y. Sera, N. Tanabe, Y. Morizawa, and Y. Suzuki, "Nano-cluster-enhanced high-performance perfluoro-polymer electrets for energy harvesting," J. Micromech. Microeng. **21**(12), 125016 (2011).
[20]F. Wang, C. Bertelsen, G. Skands, T. Pedersen, and O. Hansen, "Reactive ion etching of polymer materials for an energy harvesting device," Microelectron. Eng. **97**, 227–230 (2012).
[21]F. Wang and O. Hansen, "Invisible surface charge pattern on inorganic electrets," IEEE Electron Device Lett. **34**(8), 1047–1049 (2013).
[22]Y. Suzuki, "Recent progress in MEMS electret generator for energy harvesting," IEEJ Trans. Electr. Electron. Eng. **6**(2), 101–111 (2011).
[23]M. Wischke, M. Masur, F. Goldschmidtboeing, and P. Woias, "Electromagnetic vibration harvester with piezoelectrically tunable resonance frequency," J. Micromech. Microeng. **20**(3), 035025 (2010).
[24]C. Peters, D. Maurath, W. Schock, F. Mezger, and Y. Manoli, "A closed-loop wide-range tunable mechanical resonator for energy harvesting systems," J. Micromech. Microeng. **19**(9), 094004 (2009).
[25]Q. C. Tang and X. X. Li, "Two-stage wideband energy harvester driven by multimode coupled vibration," IEEE/ASME Trans. Mech. **20**, 115–121 (2015).
[26]I. Sari, T. Balkan, and H. Kulah, "An electromagnetic micro power generator for wideband environmental vibrations," Sens. Actuators, A **145–146**, 405 (2008).
[27]H. Kulah and K. Najafi, "Energy scavenging from low-frequency vibrations by using frequency up-conversion for wireless sensor applications," IEEE Sens. J. **8**, 261 (2008).
[28]A. M. Wickenheiser and E. Garcia, "Modeling and experimental verification of synchronized discharging techniques for boosting power harvesting from piezoelectric transducers," Smart Mater. Struct. **18**(5), 065020 (2010).
[29]F. Cottone, H. Vocca, and L. Gammaitoni, "Nonlinear energy harvesting," Phys. Rev. Lett. **102**, 080601 (2009).
[30]S. C. Lin, B. S. Lee, W. J. Wu, and C. K. Lee, "Multi-cantilever piezoelectric MEMS generator in energy harvesting," in *2009 IEEE International Ultrasonics Symposium (IUS)* (IEEE, 2009), pp. 755–758.
[31]L. Dhakar, H. Liu, F. E. H. Tay, and C. Lee, "A wideband triboelectric energy harvester," in *The 13th International Workshop on Micro and Nanotechnology for Power Generation and Energy Conversion Applications (Power MEMS 2013)*, *London, UK*, *3-6 December* (IOP Publishing, 2013), pp. 617–620.
[32]H. Liu, L. Dhakar, and C. Lee, "Ultra-broadband electromagnetic MEMS vibration energy harvesting," in *The 13th International Workshop on Micro and Nanotechnology for Power Generation and Energy Conversion Applications (Power MEMS 2013)*, *London, UK*, *3-6 December 2013* (IOP Publishing, 2013), pp. 231–234.
[33]F. Wang and O. Hansen, "Electrostatic energy harvesting device with out-of-the-plane gap closing scheme," Sens. Actuators, A **211**, 131–137 (2014).
[34]M. Bao and H. Yang, Sens. Actuators, A **136**, 3 (2007).
[35]A. Narimani, M. F. Golnaraghi, and G. N. Jazar, J. Vib. Control **10**, 1775 (2004).
[36]A. Crovetto, F. Wang, and O. Hansen, "Modeling and optimization of an electrostatic energy harvesting device," J. Microelectromech. Syst. **23**(5), 1141–1155 (2014).